

Blastic plasmacytoid dendritic cell neoplasm with immunoblastoid morphology and MYC rearrangement and overexpression



Sir,

Blastic plasmacytoid dendritic cell neoplasm (BPDCN) is a rare haematological malignancy derived from precursor plasmacytoid dendritic cells with an aggressive clinical course and a high incidence of cutaneous involvement.¹ Most cases of BPDCN have a lymphoblast- or myeloblast-like appearance characterised by a monotonous infiltrate of medium-sized cells with scant cytoplasm, finely dispersed chromatin and absent or inconspicuous nucleoli.^{1,2} The tumour cells express CD4, CD56, CD43, CD123, TCL-1 and CD303 but lack lineage-specific markers for B-, T-, or myeloid cells.¹ The initial involvement of skin and blast-like morphology are key features for recognition of this aggressive entity. However, some cases of BPDCN with variant morphological features, such as pleomorphic and centrocyte-

like neoplasms, have been reported.^{2,3} Recently, Kurt *et al.* described a rare case of BPDCN in which the neoplastic cells had prominent nucleoli associated with *MYC* rearrangement and overexpression.⁴ Here, we report a case of BPDCN with immunoblast-like morphological features associated with *MYC* rearrangement and overexpression. This case highlights the association of immunoblastoid cytomorphology and *MYC* overexpression.⁵

A 74-year-old man visited our hospital in 2004 for a skin plaque over his left upper arm. The lesion was 5 × 4 cm, well-demarcated, dusky-red, and indurated (Fig. 1A) and had been noted for 3 months with rapid enlargement. A systemic work-up was unremarkable, including laboratory data and imaging studies. A skin biopsy specimen was interpreted as BPDCN. The patient was treated with radiotherapy to a dose of 5000 cGy in 25 fractions with complete resolution, but one month later a 3 × 3 cm subcutaneous nodule recurred adjacent to the site of the initial lesion. The nodule was excised. Clinical survey revealed a stage I disease. Bone marrow aspiration and biopsy showed hypocellularity with haemopoietic components accounting for about 20–30% of the marrow space, and a myeloid/erythroid ratio of 1–2:1. No

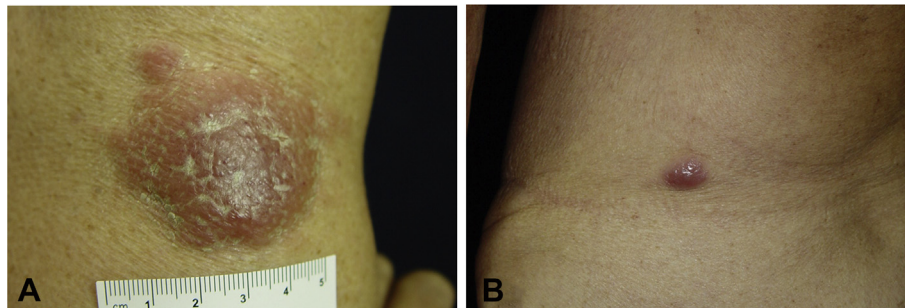


Fig. 1 Gross pictures of the multiple recurrent skin tumours. (A) The first skin lesion shows a well-demarcated, dusky-red, indurated tumour on the left upper arm, measuring 5 × 4 cm. (B) This recurrent lesion on left flank, measuring 1 cm, presents as a juicy and elastic nodule.

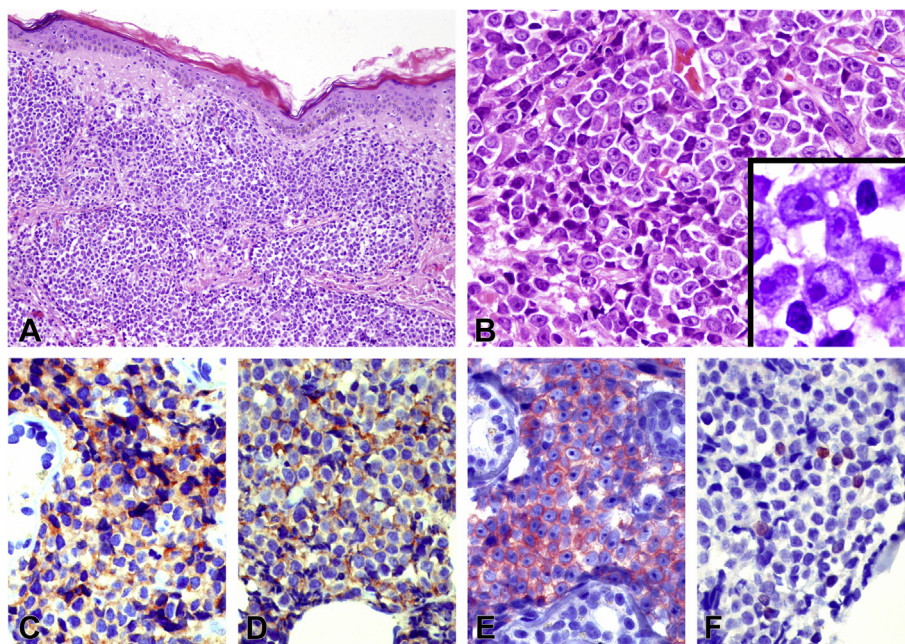


Fig. 2 Pathological findings of this tumour. (A) The dermis is infiltrated by dense tumour cells with perivascular and periadnexal accentuation. (B) On high-power field, the tumour cells are medium-sized to large and possess vesicular nuclei and moderate amount of amphiphilic cytoplasm. The prominent central nucleoli and thick nuclear membrane, reminiscent of immunoblasts, are highlighted on oil immersion (inset, 1000×). (C–F) Immunohistochemically, the tumour cells are positive for (C) CD4, (D) CD56, (E) CD123, and (F) TdT (scattered).

evidence of tumour cell involvement or myelofibrosis was found. Another course of local radiotherapy was given and the lesion was also responsive. However, three new lesions developed on his right abdomen, left flank, and right chest wall 1.5 years later (Fig. 1B). After biopsy, he received systemic chemotherapy using the COP regimen (cyclophosphamide, vincristine, prednisone) for four courses with remission for one year. Unfortunately, the tumour recurred with involvement at multiple skin sites, lymph nodes and bone marrow. The patient died of neutropenia and infection in 2008, 42 months after disease onset.

The microscopic features of the three biopsied specimens were similar. The overlying epidermis was spared with a distinct grenz zone (Fig. 2A). The dermis and subcutis contained a dense monotonous infiltrate of medium-sized to large tumour cells with immunoblast-like morphological features (Fig. 2B). Mitotic activity was brisk. Necrosis or angioinvasion was absent. Immunohistochemical studies showed that the neoplastic cells were positive for CD45/LCA, CD4, CD43, CD56, CD99, CD123, TCL1, and TdT (subset) (Fig. 2C–F) and were negative for CD3, CD20, CD34, CD45RO, CD68, CD138, myeloperoxidase, lysozyme and ALK. *In situ* hybridisation for Epstein–Barr virus encoded RNA (EBER) was negative. We also tested this case for *MYC* rearrangement by FISH and c-*MYC* expression by

immunohistochemistry in comparison with two additional BPDCN cases from our archives. Split FISH assays for *MYC* and *MYB* were performed on paraffin-embedded sections (4 µm thick) using bacterial artificial chromosome (BAC) clone-derived DNA probes, which were designed to detect rearrangements or deletions in the corresponding gene loci.⁵ As shown in Fig. 3A,B, *MYC* was rearranged (Fig. 3B inset, split) and c-*MYC* was overexpressed in contrast to other two classical cases (Fig. 3C–F). Interestingly, the third case instead showed *MYB* rearrangement (Fig. 3F inset, split).

BPDCN is clinically aggressive with a median survival of 12–16 months,⁶ and tends to present with multiple organ involvement and leukaemic dissemination. Although radiotherapy and/or chemotherapy can provide a good initial response, relapses often occur. The course seems to be related to the age of the patient at diagnosis and the duration for preleukaemic phase.⁶ It is noteworthy that when the tumour is localised in the skin, the prognosis is better, as demonstrated in the present case. Pathogenetically, gene expression profiling of BPDCN reveals aberrant activation of Notch signalling and the BCL2 and NFκB pathways.¹ Interestingly, BPDCN overexpresses c-*MYC* protein with *MYC* mutation in about 15% of cases.^{4,7,8} In a recent study with 118 cases, Sakamoto *et al.* further found that *MYC*-positive BPDCN was associated with older age, poorer outcome,

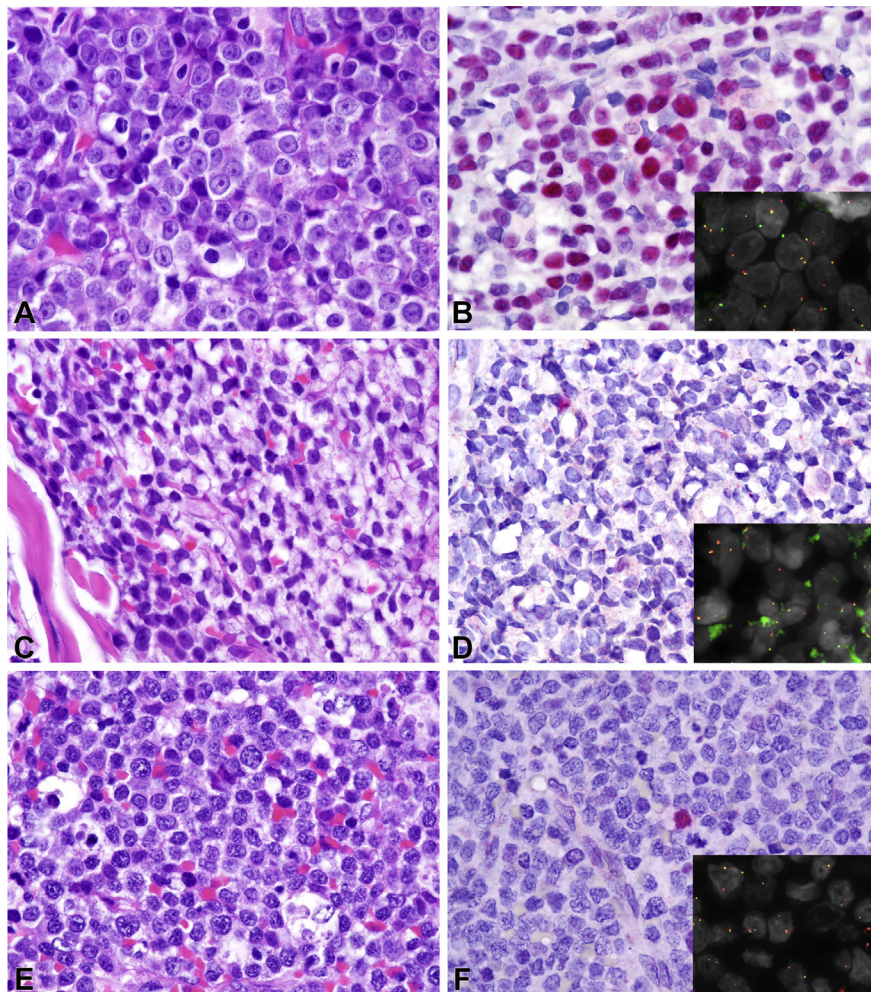


Fig. 3 (A,B) c-*MYC* protein expression and *MYC* gene rearrangement in immunoblastoid but not in (C–F) classical BPDCN. (A) This immunoblastoid variant shows immunoblast-like morphology, (B) overexpression of c-*MYC* and (B, inset) *MYC* rearrangement (split signals) in the majority of tumour cells. (C,E) In contrast, two other cases of conventional BPDCN are negative for (D,F) *MYC* expression or rearrangement but (F, inset) *MYB* rearrangement is present in the third case (split signal).

immunoblastoid cytomorphological features and *MYC* mutation compared with the *MYC*-negative BPDCN.⁵ The mechanism underlying *MYC* overexpression in BPDCN has not been clarified. The *MYC* breakpoint in BPDCN is diverse and the partner for *MYC* was not SUPT3H (6p21) in our case.⁸ As in other neoplasms with 8q24 rearrangements, overexpression of full-length *MYC* is probably ascribed to the juxtaposition of super-enhancers with *MYC* rather than generation of a particular chimaeric transcript.⁵ This may shed light on the possibility of targeting therapy given that bromodomain inhibition can induce potent anti-proliferation in cases of *MYC*-dependent BPDCN.⁵

Acknowledgements: The authors are grateful to Dr L. Jeffrey Medeiros (Department of Hematopathology, The University of Texas MD Anderson Cancer Center, Houston, Texas) for critical review of the manuscript.

Conflicts of interest and sources of funding: The authors state that there are no conflicts of interest to disclose.

Kung-Chao Chang¹, Julia Yu-Yun Lee², Kana Sakamoto³, Satoko Baba³, Kengo Takeuchi^{3,4}

¹Department of Pathology, National Cheng Kung University Hospital, College of Medicine, National Cheng Kung University, Tainan, Taiwan; ²Department of Dermatology, National Cheng Kung University Hospital, College of Medicine, National Cheng Kung University, Tainan, Taiwan; ³Pathology Project for Molecular Targets, Cancer Institute, Japanese Foundation for Cancer Research, Tokyo, Japan; ⁴Division of Pathology, Cancer Institute, Japanese Foundation for Cancer Research, Tokyo, Japan

Contact Kung-Chao Chang.

E-mail: changkc@mail.ncku.edu.tw

1. Swerdlow SH, Campo E, Harris NL, et al. *WHO Classification of Tumours of Haematopoietic and Lymphoid Tissues*. Revised 4th ed. Lyon: IARC, 2017; 174–7.
2. Cota C, Vale E, Viana I, et al. Cutaneous manifestations of blastic plasmacytoid dendritic cell neoplasm—morphologic and phenotypic variability in a series of 33 patients. *Am J Surg Pathol* 2010; 34: 75–87.
3. Chu C, Rudnick EW, Motaparthy K. Blastic plasmacytoid dendritic cell neoplasm with centrocyte-like morphology clinically simulating a melanocytic nevus. *J Cutan Pathol* 2018; 45: 249–53.
4. Kurt H, Khoury JD, Medeiros LJ, et al. Blastic plasmacytoid dendritic cell neoplasm with unusual morphology, *MYC* rearrangement and TET2 and DNMT3A mutations. *Br J Haematol* 2018; 181: 305.
5. Sakamoto K, Katayama R, Asaka R, et al. Recurrent 8q24 rearrangement in blastic plasmacytoid dendritic cell neoplasm: association with immunoblastoid cytomorphology, *MYC* expression, and drug response. *Leukemia* 2018; May 23: (Epub ahead of print).
6. Pagano L, Valentini CG, Grammatico S, et al. Blastic plasmacytoid dendritic cell neoplasm: diagnostic criteria and therapeutic approaches. *Br J Haematol* 2016; 174: 188–202.
7. Boddu PC, Wang SA, Pemmaraju N, et al. 8q24/*MYC* rearrangement is a recurrent cytogenetic abnormality in blastic plasmacytoid dendritic cell neoplasms. *Leuk Res* 2018; 66: 73–8.
8. Nakamura Y, Kayano H, Kakegawa E, et al. Identification of SUPT3H as a novel 8q24/*MYC* partner in blastic plasmacytoid dendritic cell neoplasm with t(6;8)(p21;q24) translocation. *Blood Cancer J* 2015; 5: e301.

DOI: <https://doi.org/10.1016/j.pathol.2018.09.058>

FDG-PET/CT findings, the vital clue to rare diagnosis of herpes simplex virus lymphadenitis simulating Richter transformation



Sir,

A 55-year-old male born in Vietnam, with known chronic lymphocytic leukaemia (CLL) monitored without therapy, presented with new fevers, night sweats, loss of weight and retroperitoneal lymphadenopathy. He was subsequently diagnosed with herpes simplex virus (HSV) lymphadenitis based on histopathological findings. The patient denied any focal symptoms and had no localising signs to point to a source of fever. There were no typical features of disseminated HSV (hepatitis, pneumonitis or disseminated skin lesions), nor did the patient have any active lesions of oral or genital herpes. The patient reported a distant history of orolabial HSV but no genital lesions. A septic screen including blood cultures, urine culture and chest X-ray were negative. Given the differential for this patient's presentation was a Richter transformation (transformation of CLL into diffuse large B-cell lymphoma, an aggressive condition requiring active treatment¹), an FDG-PET/CT was ordered. This demonstrated the previously known sites of cervical, hilar and mediastinal lymphadenopathy secondary to CLL to be of low FDG-avidity and only mild diffuse splenic uptake, however there were new enlarged retroperitoneal lymph nodes with high FDG-avidity [maximum standard uptake value (SUVmax) 6.43] (Fig. 1). There was an area of photopenia within the centre of the nodal mass consistent with necrosis. A diagnostic laparotomy was performed and a biopsy of the retroperitoneal lymph nodes, with the likely differential diagnoses of Richter transformation and tuberculosis. The biopsy revealed a focal necrotising granulomatous process with central necrosis containing giant cells and histiocyte debris (Fig. 2). Within the necrotic areas, scattered epithelioid cells showed classic nuclei and occasional multinucleated giant cells with margined nuclei resembling

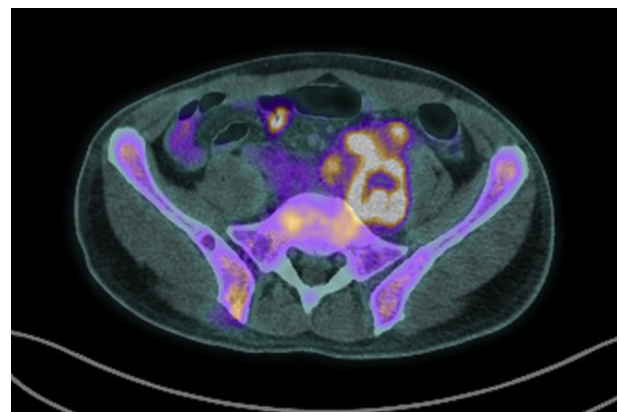


Fig. 1 A fused image of FDG-PET/CT demonstrating avid retroperitoneal lymphadenopathy with a pronounced area of central necrosis.